JOURNAL OF SOLID STATE CHEMISTRY 49, 219–231 (1983)

Brownmillerite-Type Microdomains in the Calcium Lanthanum Ferrites: $Ca_xLa_{1-x}FeO_{3-y}$

I. $\frac{2}{3} < x < 1$

M. A. ALARIO-FRANCO,[1] J. M. GONZALEZ-CALBET, AND M. VALLET-REGI

Departamento de Química Inorgánica, Facultad de Ciencias Químicas, Universidad Complutense, Madrid-3, and Instituto de Química Inorgánica "Elhuyar" CSIC, Serrano 113, Madrid-6, Spain

AND J. C. GRENIER

Laboratoire de Chimie du Solide du CNRS, Université de Bordeaux I, 351, cours de la Libération, 33405 Talence Cedex, France

Received January 13, 1983, and in revised form April 19, 1983

The study by high resolution electron microscopy and electron diffraction of several oxidized samples of the calcium lanthanum ferrites $Ca_xLa_{1-x}FeO_{3-y}$, with different values of x and y, prepared at high temperatures in air, shows the existence of a *microdomain texture* in which brownmillerite-type microdomains with a volume of $\sim 10^6$ Å^3 are intergrowth within a $Ca_2LaFe_3O_8$ substructure. This situation was not detected by conventional powder X-ray methods, where a simple cubic perovskite unit cell with constant parameters was observed ($a = 3.849(1)$ Å for $x = 0.8$ and $a = 3.848(1)$ Å for $x = 0.9$). Electron micrograph images of the microdomain texture show that fringe periodicity is very regular suggesting that the oxygen excess is situated in the domain walls.

Introduction

We have recently shown that compositional variations in perovskite related oxides can be associated with three-dimensional microdomain formation (*1, 2*). These microdomains have a unit cell that is a multiple of a cubic perovskite subcell and the multiplicity occurs at random in one of the three cubic unit cell directions in each domain. These types of textured materials have been found in some samples of the solid solution $Sr_xNd_{1-x}FeO_{3-y}$ (*1*) and in calcium lanthanum ferrite (*2*) $Ca_{2/3}La_{1/3}FeO_{8/3}$ oxidized at high temperature. These are the first examples of a new way of accommodating compositional variations in solids; so a deeper study of this type of nonstoichiometry is obviously needed.

The study by TEM and ED of several samples of the $Ca_xLa_{1-x}FeO_{3-y}$ ($\frac{2}{3} < x < 1$) annealed at low oxygen pressures and moderate temperatures (~1100°C) has shown (*3*) that these materials are constituted by disordered intergrowths between the members $x = \frac{2}{3}$ ($Ca_2LaFe_3O_8$) and $x = 1$ ($Ca_2Fe_2O_5$). Figure 1 shows a typical example, corresponding to the reduced $x = 0.8$ sample (*3*). Brownmillerite-type regions, marked B, characterized by a $d \simeq 7.4$ Å spacing are intergrown with other regions, characterized by a $d' \simeq 11.3$ Å spacing corresponding to $Ca_2LaFe_3O_8$, marked G. The corresponding electron diffraction pattern,

[1] To whom all correspondence should be addressed.

0022-4596/83 $3.00

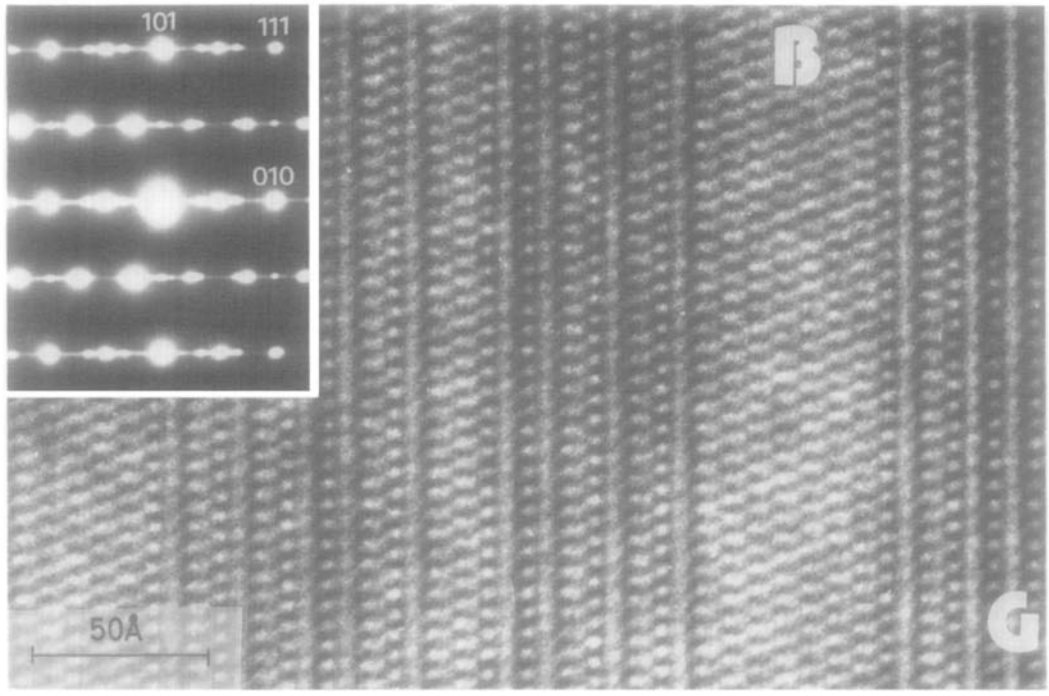

FIG. 1. High resolution electron micrograph of the LT reduced $x = 0.8$ sample. The inset shows the corresponding electron diffraction pattern indexed on the cubic perovskite basis. The presence of a disordered intergrowth between $Ca_2Fe_2O_5$ (B) and $Ca_2LaFe_3O_8$ (G) is evident. Zone axis $[10\bar{1}]_c <> [100]_G$.

seen in the inset, shows the superposition of the patterns of both those oxides.

In this paper we report and discuss the results of a study of the high temperature oxidized materials corresponding to the same compositions: $\frac{2}{3} < x < 1$.

Experimental

Samples were prepared by heating the appropriate amounts of $CaCO_3$, La_2O_3, and Fe_2O_3, of Analar quality, at 1400°C for 1 day and fast-quenched to room temperature.

The average oxidation state of iron was determined by chemical analysis with $K_2Cr_2O_7$ solution after dilution in 3 *N* HCl with an excess of Mohr's salt.

X-Ray diffraction data were obtained on a Siemens D-500 diffractometer.

Specimens for the electron microscope were ultrasonically dispersed in *n*-butanol and then mounted on carbon-coated microgrids. Observations were made in a Siemens Elmiskop 102 electron microscope equipped with a ± 45° tilt goniometer stage and operated at 100 kV. Focusing conditions close to the optimum defocus (Scherzer) conditions (*4*) were employed.

Results

The samples annealed in an argon atmosphere ($pO_2 < 10^{-6}$ atm) at 1100°C (LT samples) did show the existence of disordered intergrowths between $Ca_2Fe_2O_5$ and $Ca_2LaFe_3O_8$ (*3*). Chemical analysis of those samples indicated the absence of Fe(IV).

When the samples were prepared at 1400°C in air (HT samples) a totally differ-

ent situation was present. Chemical analysis indicated the compositions $Ca_{0.8}La_{0.2}FeO_{2.665}$ and $Ca_{0.9}La_{0.1}FeO_{2.615}$ corresponding to about the same amount of Fe(IV) in both samples: 12.9 ± 0.1 and 13.0 ± 0.1%, respectively. The corresponding X-ray diffraction powder patterns were formed by relatively broad peaks, indexable on a cubic perovskite-type unit cell, and having indistinguishable unit cell parameters: a = 3.849(1) Å for x = 0.8 and a = 3.848(1) Å for x = 0.9. As reported previously (2) the oxidized high temperature $x = \frac{2}{3}$ sample, $Ca_{0.66}La_{0.33}FeO_{2.745}$, with an Fe(IV) content of 15.6%, has a cubic subcell parameter a = 3.848(3) Å. Here also the electron microscopy and diffraction data were much more illustrative of the real situation. In the first instance, no *simple* disordered intergrowth was found.

The large majority of the observed crystals of both HT samples did show electron diffraction patterns analogous to that shown in Fig. 2a which, on a first approximation, can be indexed in a perovskite cell doubled in, at least, two directions. However, the corresponding electron micrograph, Fig. 2b, shows that the crystal is formed by a kind of patchwork in which fringes with a spacing of 7.4 Å are periodic in one of two directions; these directions are either a_c[2] or b_c according with the indexing of Fig. 2a. There are also regions, such as that marked by an arrow, in which no fringes are seen. A *microdomain texture* is then present in a situation which is similar to that found previously in analogous anion deficient perovskites (*2*).

However, there is an apparent conflict between the information contained in Figs. 2a and b since, if it were really a perovskite unit cell doubled in two perpendicular directions, a ~7.6 × 7.6 Å square net of crossing fringes should be visible in each domain; however, fringes are only visible in one dimension in each domain. In order to clear up the situation, a series of tilts were successively performed along the a_c^* and b_c^* axes of the same crystal. Before describing the results of these tilting experiments, we will note that, in every crystal, for a giving tilting angle, the same pattern was obtained on tilting along a_c^* or b_c^*.

Figure 3a shows the $[10\bar{1}]_c$ zone axis, obtained after a tilt of 45° around b_c^*. It is clear that this pattern does not fit to a perovskite unit cell doubled in two directions. In fact it can simply be indexed on the basis of a brownmillerite type unit cell along the $[100]_B$ zone axis. An schematic representation of this section of the reciprocal lattice is given in Fig. 3b; the brownmillerite diffraction maxima have been indicated by open circles within a cubic perovskite reciprocal cell (dark circles). As it is known, the brownmillerite structure can be considered as a fourfold superstructure of the perovskite structure. However, as in the space group *Pnma*, corresponding to brownmillerite, reflections $(0kl)$ are allowed if $k + l = 2n$, only the reflections with both indexes odd or both even appear in the $[100]_B$ zone (Fig. 3b).

Figure 4a shows the $[10\bar{2}]_c$ zone axis electron diffraction pattern, indexed on the perovskite cell and schematically represented in Fig. 4b. Although the presence of a spot at $(1\ 0\ \frac{1}{2})_c$ seems to suggest that the third perovskite cell axis, c_c^*, is also doubled, indicating that there is a third group of domains, the presence of the spot located at $(\frac{1}{2}\ \frac{1}{2}\ \frac{1}{4})_c$ and $(\frac{3}{2}\ \frac{1}{2}\ \frac{3}{4})_c$, and equivalent positions implies that in the c_c^* direction there is also a brownmillerite type superstructure. There are also very weak and diffuse diffraction maxima at $(1\ \frac{1}{2}\ \frac{1}{2})_c$ and equivalent positions that we will consider below.

Figure 5a shows the $[10\bar{3}]_c$ zone axis, indexed on the cubic basis, and schematically plotted in Fig. 5b. The majority of the spots

[2] Subindex c refers to the cubic perovskite unit cell. Subindexes B and G refer to the brownmillerite and $Ca_2LaFe_3O_8$-type unit cells, respectively.

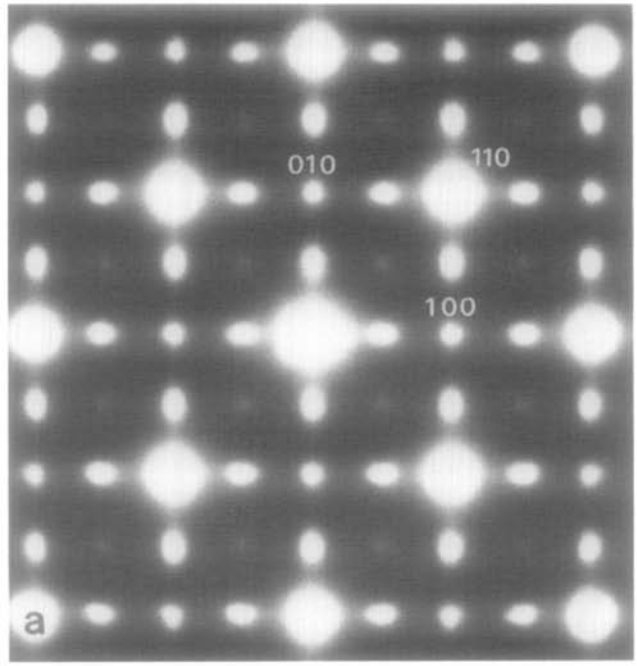

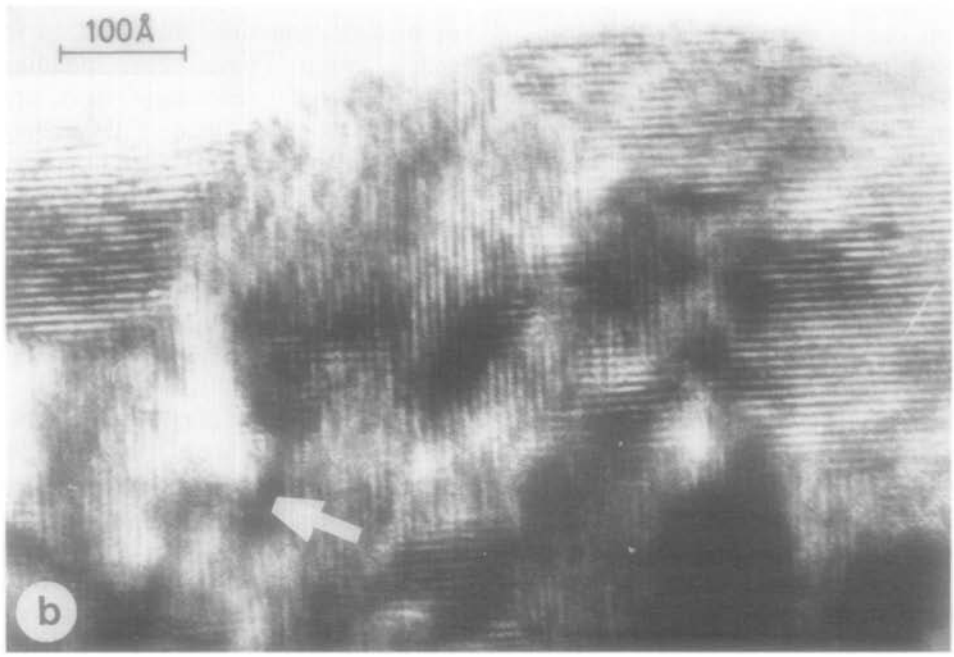

FIG. 2. (a) Typical electron diffraction pattern of the high temperature samples. Zone axis $[001]_c$. (b) Electron micrograph corresponding to the above zone axis. The presence of a microdomain texture is obvious. Fringe separation within each domain is ~7.4 Å.

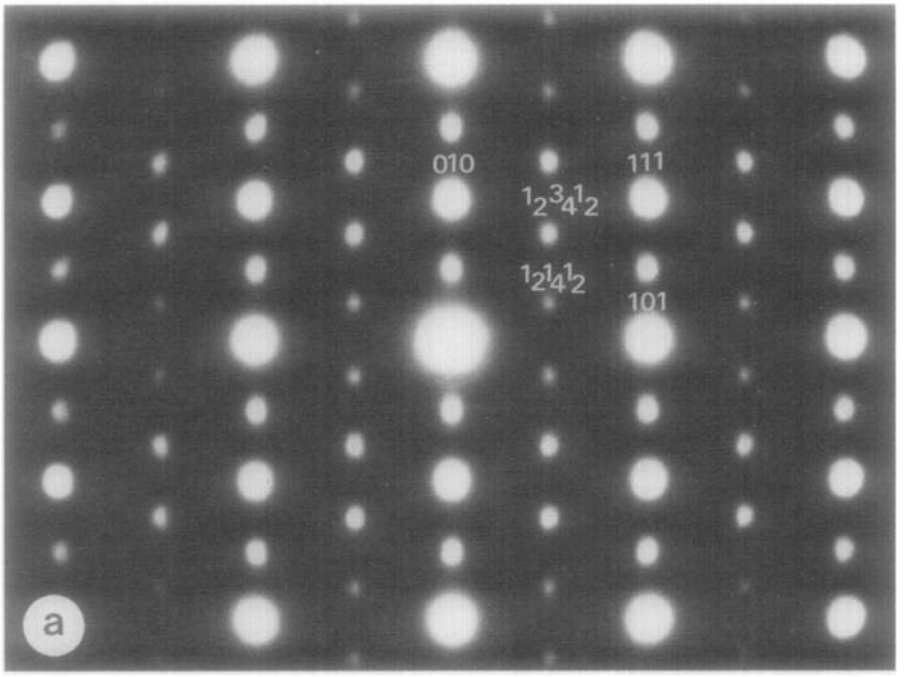

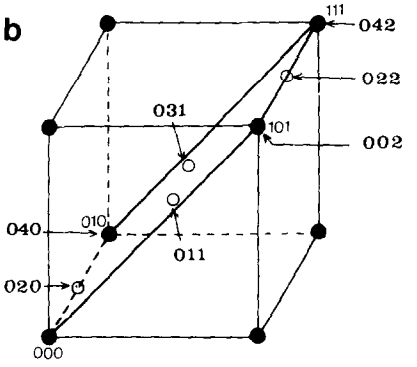

FIG. 3. (a) Electron diffraction pattern of the HT sample. Zone axis $[10\bar{1}]_c <> [100]_B$. (b) Schematic representation of the above pattern within a reciprocal net corresponding to the perovskite substructure. Arrowed indexes correspond to brownmillerite type cell.

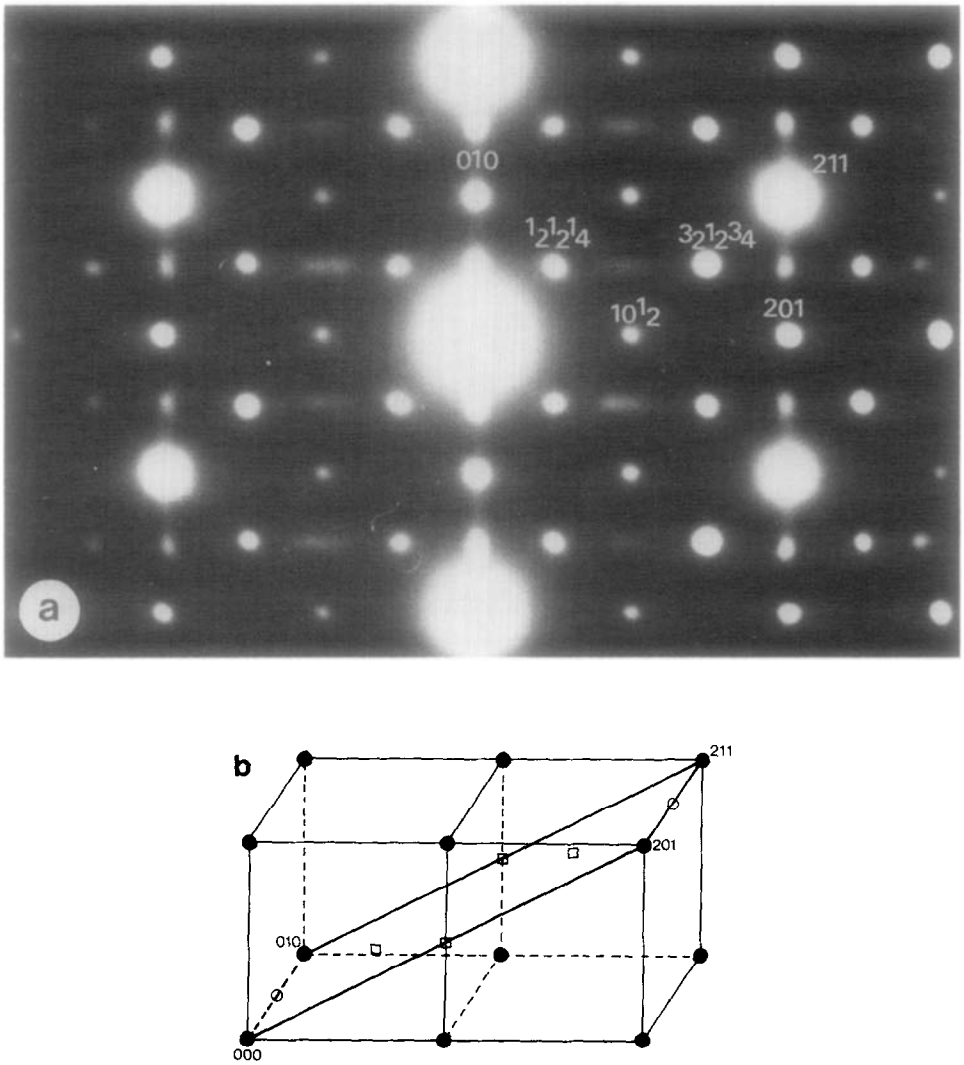

FIG. 4. (a) Electron diffraction pattern of the HT sample. Zone axis $[10\bar{2}]_c$. (b) Schematic representation of the above pattern within a reciprocal net corresponding to the perovskite substructure.

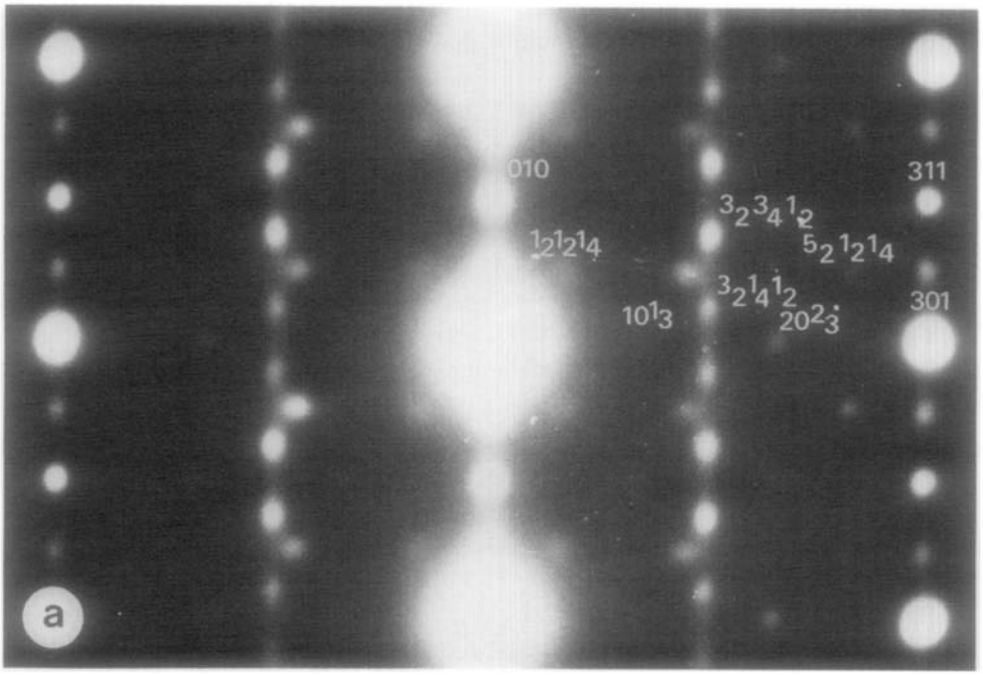

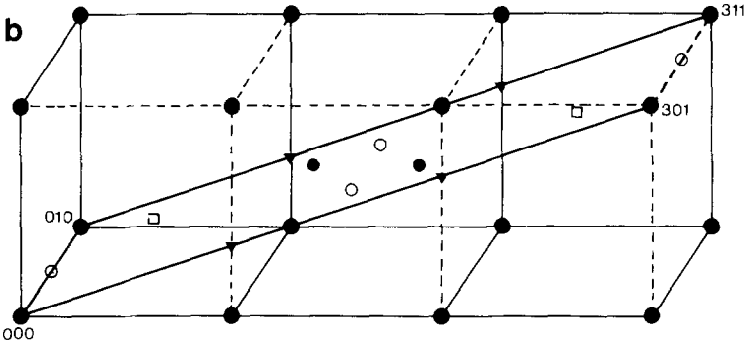

FIG. 5. (a) Electron diffraction pattern of the HT sample. Zone axis $[10\bar{3}]_c$. (b) Schematic representation of the above pattern within a reciprocal net corresponding to the perovskite substructure.

in this pattern can be indexed by the juxtaposition of three brownmillerite-like reciprocal nets differing in the orientation of the long b_B^* axis, as schematized in Fig. 6a. It appears then that these solids have a three-dimensional microdomain texture, reminiscent of that found in the calcium lanthanum ferrite.

Nevertheless, as stated above, there are more spots in Fig. 5a than diffraction maxima expected from the simple juxtaposition of the three reciprocal nets shown in Fig. 6a. Note, in particular, the diffracted intensity located at $(1\ 0\ \frac{1}{3})_c$, $(2\ 0\ \frac{2}{3})_c$, and equivalent positions on Fig. 5a.

Coming back to the $[001]_c$ zone axis and tilting around the a_c^* axis, it was observed that the $[01\bar{1}]_c$ pattern was identical to the $[10\bar{1}]_c$ pattern of Fig. 3a. Likewise, the $[01\bar{3}]_c$ and $[10\bar{3}]_c$ patterns were identical. However, although the $[01\bar{2}]_c$ diagram was identical with the $[10\bar{2}]_c$ pattern (Fig. 4a), they both differ from the $[20\bar{1}]_c$ diagram shown in Fig. 7a. The essential difference resides in the spot located at $(\frac{1}{2}\ \frac{1}{2}\ 1)_c$ which does not have counterparts in the $[01\bar{2}]_c$ and $[20\bar{1}]_c$ zones (compare Figs. 4b and 7b) and which obviously corresponds with the spot appearing at the center of the basal reciprocal plane of Fig. 2a.

The ensemble of these observations suggests that the complete reciprocal lattice corresponding to the high temperature $x = 0.8$ and $x = 0.9$ calcium lanthanum ferrites

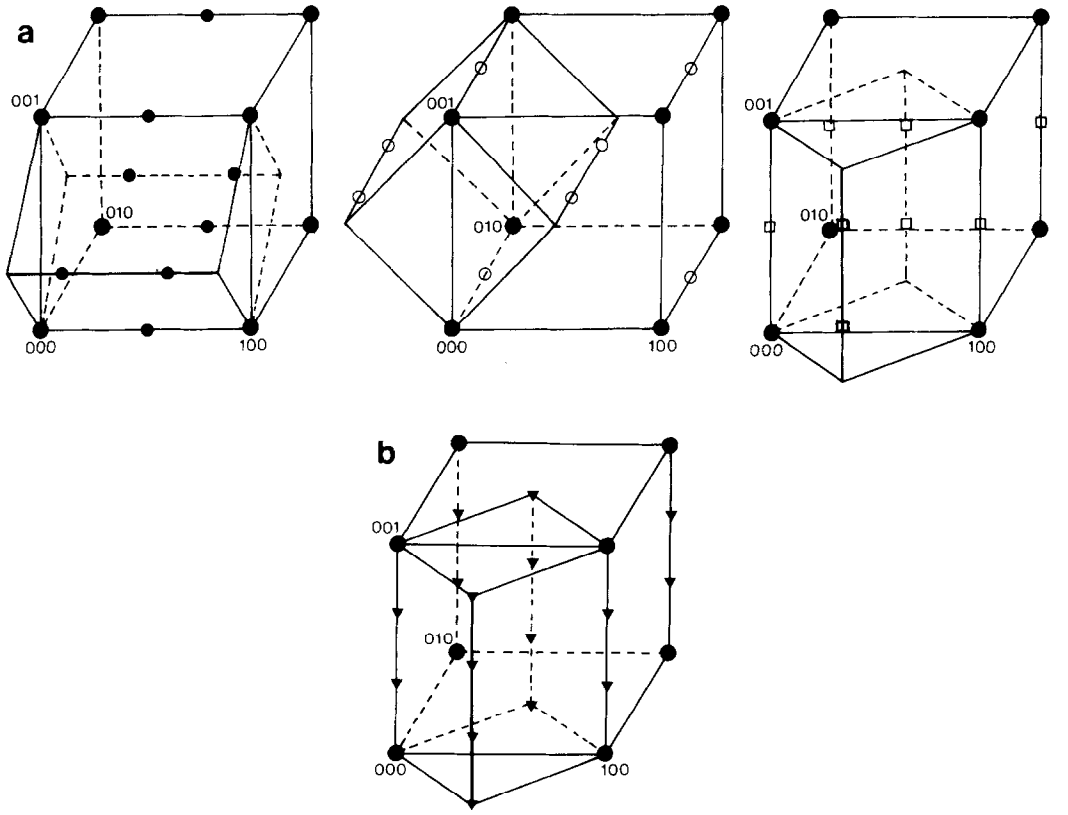

FIG. 6. Schematic representation of (a) the tree brownmillerite-type reciprocal nets and (b) the $Ca_2LaFe_3O_8$-like reciprocal net forming the reciprocal net of the HT oxidized sample (see text for details).

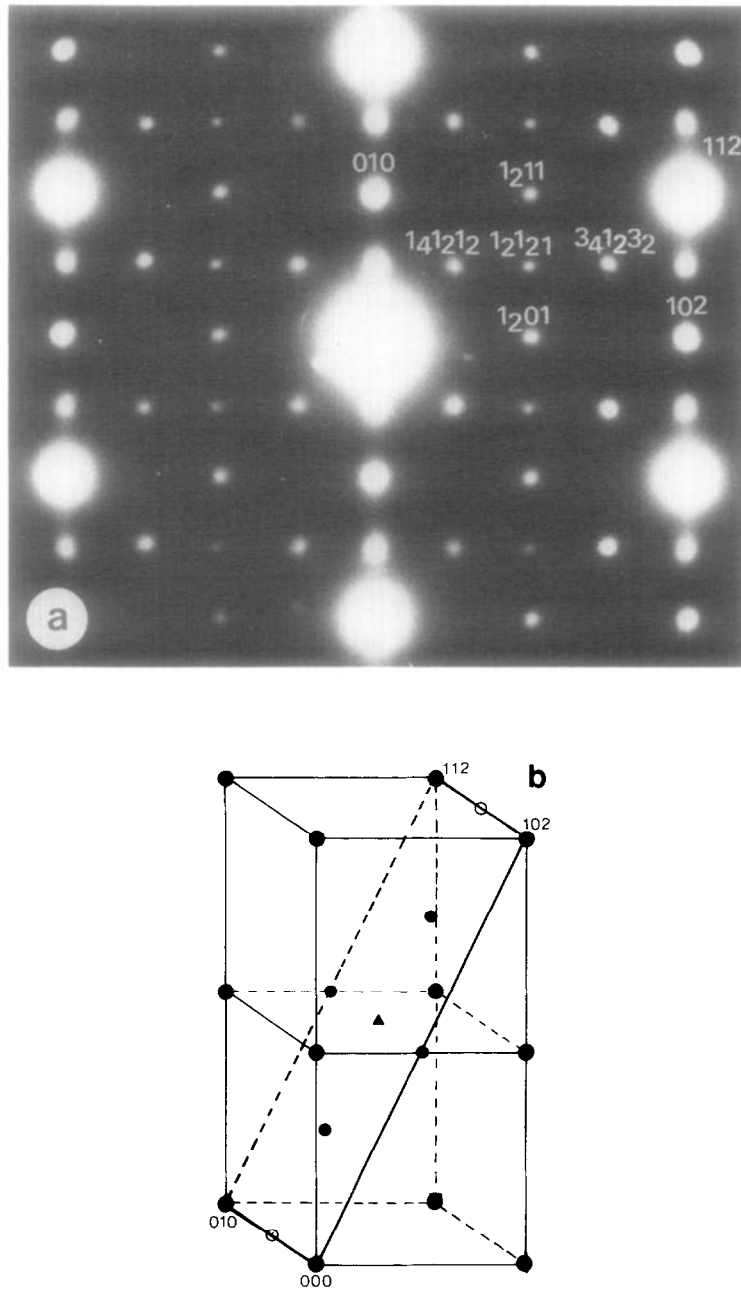

FIG. 7. (a) Electron diffraction pattern of the high temperature sample. Zone axis $[20\bar{1}]_c$. (b) Schematic representation of the above pattern within a reciprocal net of the perovskite substructure (compare with $[10\bar{2}]_c$ in Fig. 4).

is as depicted in Fig. 8 and results, in fact, from the juxtaposition of four different reciprocal nets:

The three brownmillerite-like nets shown in Fig. 6a correspond each one to a set of domains: set α for the domains having b^*_β

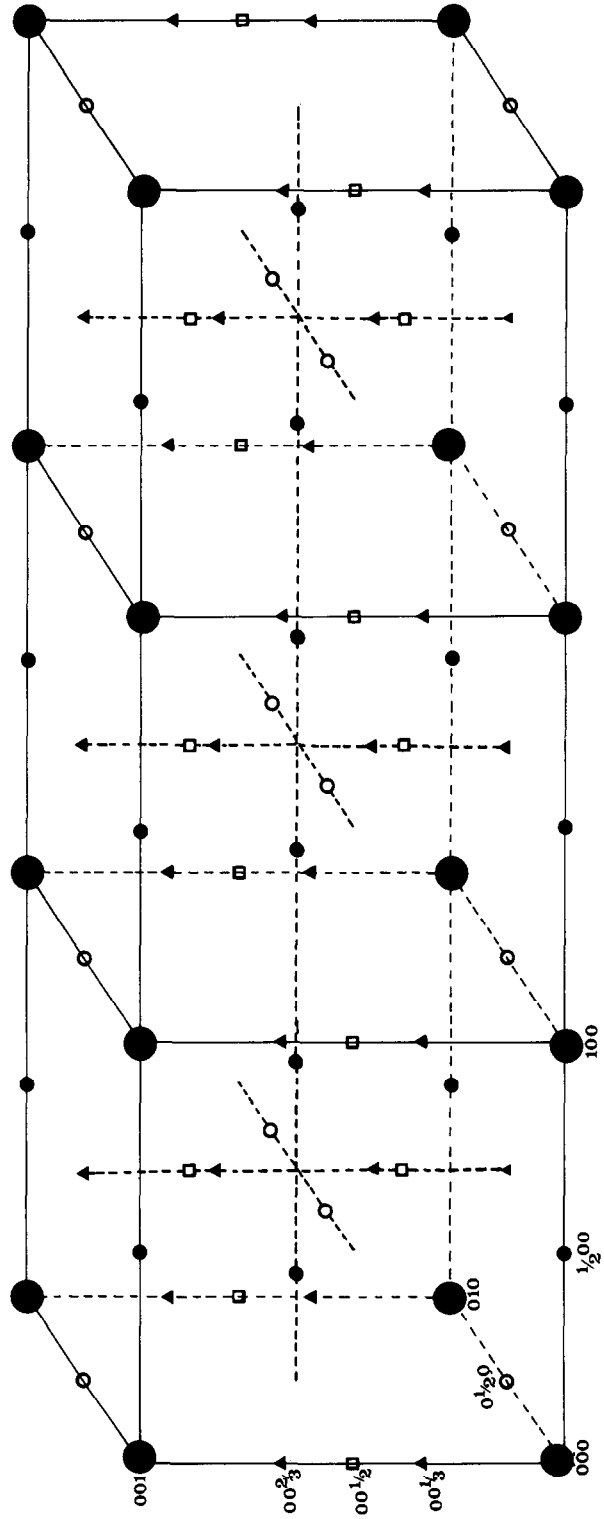

FIG. 8. Complete reciprocal lattice of the high temperature samples. It is composed by the juxtaposition of the *four* reciprocal nets shown in Fig. 6.

Perovskite (c)	$a_c \times a_c \times a_c$	
Brownmillerite (B)	$4a_c \times a_c\sqrt{2} \times a_c\sqrt{2}$	set α
	$a_c\sqrt{2} \times 4a_c \times a_c\sqrt{2}$	set β
	$a_c\sqrt{2} \times a_c\sqrt{2} \times 4a_c$	set γ
$Ca_2LaFe_3O_8$ (G)	$a_c\sqrt{2} \times a_c\sqrt{2} \times 3a_c$	

parallel to a_c^*, set β for those domains having b_B^* parallel to b_c^* and set γ for the microdomain set with b_B^* parallel to c_c^*. There is still another net, shown in Fig. 6b, corresponding to a $Ca_2LaFe_3O_8$-like reciprocal lattice whose b_G^* axis is coincident with the c_c^* direction of the cubic perovskite substructure and consequently it is also parallel to the b_B^* axis of the γ set of domains. It is to be stressed that the diffraction maxima corresponding to this last net are much weaker than those corresponding to the other three sets.

The weak elongated reflections appearing at $(1\ \frac{1}{2}\ \frac{1}{2})_c$ and equivalent positions in Fig. 4a (referred to above) can be interpreted as due to the intersection of the Ewald sphere with the spots located at $(\frac{3}{4}\ \frac{1}{2}\ \frac{1}{2})_c$ and $(\frac{5}{4}\ \frac{1}{2}\ \frac{1}{2})_c$ corresponding to the brownmillerite-type set of domains having their b_B^* axis parallel to a_c^*.

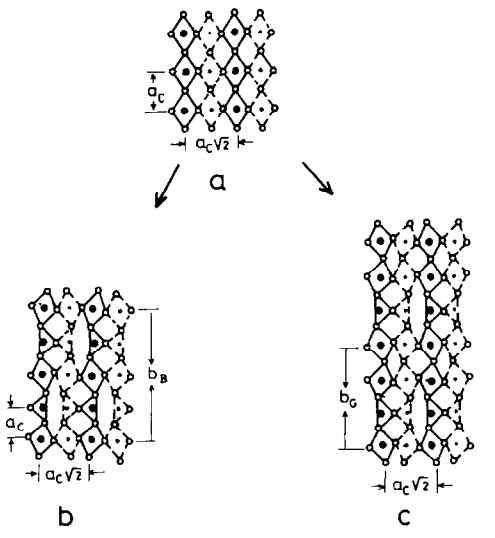

FIG. 9. Projection along an equivalent axis of the three structures forming the calcium lanthanum ferrites studied in the present work. (a) Perovskite along $[10\bar{1}]_c$. (b) $Ca_2Fe_2O_5$ along $[100]_B$ <> $[10\bar{1}]_c$. (c) $Ca_2LaFe_3O_8$ $[100]_G$ <> $[10\bar{1}]_c$.

Discussion

The above results clearly show the important differences existing between the reduced and oxidized forms of the calcium lanthanum ferrites $Ca_xLa_{1-x}FeO_{3-y}$. In the composition range studied in the present work $\frac{2}{3} < x < 1$, the reduced samples are formed by the disordered intergrowth between the end members of this range, $x = \frac{2}{3}$: $Ca_2LaFe_3O_8$ and $x = 1$: $Ca_2Fe_2O_5$. The facility of this intergrowth can certainly be attributed to the close relationship existing between the structures of the end members. Both $Ca_2Fe_2O_5$ and $Ca_2LaFe_3O_8$ can be considered as perovskite superstructures and can formally be deduced from the perovskite structure by subtracting a certain amount of oxygen. This modifies the coordination number of both cations and a number of octahedra are converted into tetrahedra: one out of three in $Ca_2LaFe_3O_8$ and one out of two in $Ca_2Fe_2O_5$.

Figure 9 shows projections of the sequence of polyhedra forming the three structures. The perovskite structure is projected along $[10\bar{1}]_c$, the brownmillerite type structure along a_B, and the $Ca_2LaFe_3O_8$ structure along a_G so as to make the three projections comparable. We point out that the structure of $Ca_{2/3}La_{1/3}FeO_{8/3}$ is not yet known but there are good reasons to accept, in a first approximation, the model shown in Fig. 9c (*3*). It can be observed, in Fig. 9b, that due to relative orientation of consecutive tetrahedra along the b_B axis, the brownmillerite supercell is four times the perovskite subcell along this direction.

As a result of this close structural relationship, the a and c parameters of both superstructures are very similar: a_B = 5.4253(5) Å $\simeq a_c\sqrt{2} \simeq a_G$ = 5.464(3) Å, and c_B = 5.5980(5) Å $\simeq a_c\sqrt{2} \simeq c_G$ = 5.563(3) Å, while the b axis, which is the intergrowth axis, is different: b_B = 14.7687(17) $\simeq 4a_c$ and b_G = 11.29(1) Å $\simeq 3a_c$ (a_c being the simple cubic perovskite parameter, a_c = 3.9 Å).

An essential consequence of this analogy

is that, under reducing conditions, that is, in the absence of Fe(IV), compositional variations by means of anion deficiency in the perovskite structure, are controlled by the Ca/La ratio, and are accommodated by changes in the relative amounts of the end members. In fact the studied samples have compositions corresponding to

$$x = 0.8 \text{ ``}Ca_{0.8}La_{0.2}FeO_{2.60}\text{''} <> Ca_2Fe_2O_5 + Ca_2LaFe_3O_8$$

and

$$x = 0.9 \text{ ``}Ca_{0.9}La_{0.1}FeO_{2.55}\text{''} <> 3.5\ Ca_2Fe_2O_5 + Ca_2LaFe_3O_8.$$

It is clear, however, that this type of solid cannot simply be considered as "phase mixtures." As Fig. 1 shows, local compositions are very heterogeneous and difficult to define in those cases, even if classic chemical analysis can provide an average chemical formula.

On the other hand, the oxidized high temperature samples do have a far more complex nature. According to the electron microscopy and diffraction evidence shown above, the majority of the crystals of both the $x = 0.8$ and $x = 0.9$ samples contain a brownmillerite-like microdomain texture and a certain amount of phase closely related to $Ca_2LaFe_3O_8$. We have then a situation that resembles the one observed in the oxidation of $Ca_2LaFe_3O_8$ to $Ca_2LaFe_3O_{8.235}$ (*2*) when three sets of microdomains of a modified LT phase were observed in the HT solid. There are however important differences between these two cases.

In the first instance the structure within each domain is in the present case brownmillerite-like, see Fig. 2b, i.e., in each set of domains the unit cell shows a fourfold superstructure of the perovskite subcell, but the long b_B axis alternates randomly in one of the three space dimensions, i.e., in set α the unit cell is $4a_c \times a_c\sqrt{2} \times a_c\sqrt{2}$, in set β: $a_c\sqrt{2} \times 4a_c \times a_c\sqrt{2}$, and in set γ: $a_c\sqrt{2} \times a_c\sqrt{2} \times 4a_c$. The observed reciprocal lattice suggests that, in each set of domains, the unit cell is, at least metrically, tetragonal while normal brownmillerite is in fact orthorhombic (*5–8*). This was also the case in the HT oxidized form of the $Ca_2LaFe_3O_8$ (*2*).

Another interesting observation is that the brownmillerite-type domains appear to be somewhat bigger than those observed in the $Ca_2LaFe_3O_8$ where a volume of the order of 200–1000 unit cells per microdomain was estimated from the electron micrographs. In the present case, there appears to be a marked heterogeneity in the domain size and is really difficult to have a precise idea of the actual domain dimensions but the domain size is of the order of 15 unit cells in the b_B direction with a corresponding domain volume of ~3300 unit cells, i.e., $\sim 10^6$ Å^3 or about three times the maximum microdomain volume estimated in $Ca_2LaFe_3O_{8+x}$.

Since, as observed in Fig. 2b, fringe separation within each domain is very regular, we believe that in this type of microdomain textured solids the oxygen excess must be located in the domain walls. Consequently, compositional variations in the anion sublattice should be reflected in the domain size and a greater domain size implies a smaller oxygen excess; at the limit, an only domain would correspond to the dicalcium ferrite, with no oxygen excess: $Ca_2Fe_2O_5$. On the other hand, an infinite number of domains of an infinitely small size would correspond to the perovskite structure, with no oxygen deficiency: ABO_3.

There is still a problem with the present HT solids. As indicated previously, the complete reciprocal lattice was composed of four different individuals. We have been referring so far to three of them, those corresponding to the three brownmillerite-type microdomain sets. The fourth has the tetragonal variant (*2*) of the $Ca_2LaFe_3O_8$

structure. We have not been able to observe it in the present case by electron microscopy and all the images obtained, corresponding to these "multiple solids," were in orientations that do not allow an identification of that phase. For this we need electron diffraction patterns in the $[010]_c$ zone axis. Until we find them we can refer loosely to this $Ca_2LaFe_3O_8$ as the matrix where the brownmillerite microdomains are intergrowth. Alternatively and in view of their lower diffracted intensity we can consider it as a relic of the LT solids, the matrix being the perovskite-type substructure. It is obvious that an extra effort is required in those solids, in particular in connection with the structure of the domain walls.

In any case, the formation of three-dimensional microdomains in those ferrites seems to be quite a general phenomenon, this being the third example so far found.

Acknowledgments

We thank Luis Puebla and Alfonso García for technical assistance.

References

1. M. A. ALARIO-FRANCO, J. C. JOUBERT, AND J. P. LEVY, *Mater. Res. Bull.* **17,** 733 (1982).
2. M. A. ALARIO-FRANCO, M. J. R. HENCHE, M. VALLET, J. M. G. CALBET, J. C. GRENIER, A. WATTIAUX, AND P. HAGENMULLER, *J. Solid State Chem.* **45** (1982).
3. J. M. GONZALEZ-CALBET, M. VALLET-REGÍ, M. A. ALARIO-FRANCO, AND J. C. GRENIER, *Mat. Res. Bull* **18,** 285 (1983).
4. M. A. O'KEEFE AND P. BUSECK, *Trans. Amer. Cryst. Assoc.* **15,** 27 (1979).
5. E. F. BERTAUT, L. BLUM, AND A. SAGNIERES, *Acta Crystallogr.* **12,** 149 (1959).
6. A. A. COLVILLE, *Acta Crystallogr. B* **26,** 1469 (1970).
7. J. BERGGREN, *Acta Chem. Scand.* **25**(10), 3616 (1971).
8. A. A. COLVILLE, *Acta Crystallogr. B* **27,** 2311 (1971).